Optics & Laser Technology 167 (2023) 109777

Contents lists available at ScienceDirect

Optics and Laser Technology

journal homepage: www.elsevier.com/locate/optlastec

Full length article

Picosecond laser writing of highly conductive copper micro-contacts from deep eutectic solvents

Dmitry Shestakov [a], Evgeniia Khairullina [b,d], Andrey Shishov [b], Soslan Khubezhov [c], Sergey Makarov [c], Ilya Tumkin [b,*], Lev Logunov [a,*]

[a] Department of Physical Electronics and Technology, Saint Petersburg Electrotechnical University "LETI", 197376 Saint Petersburg, Russia
[b] Institute of Chemistry, Saint Petersburg State University, 7/9 Universitetskaya nab., St. Petersburg 199034, Russia
[c] School of Physics and Engineering, ITMO University, Lomonosova, 9, Saint-Petersburg 191002, Russia
[d] SCAMT Laboratory, ITMO University, Lomonosova, 9, Saint-Petersburg 191002, Russia

ARTICLE INFO

Keywords:
Direct laser writing
Copper
Light-emitting devices
Deep eutectic solvent
Ultrashort laser pulses

ABSTRACT

Techniques for local metallization of dielectric materials are widely applied for the design of various electronic devices. One of the most flexible methods for local contact fabrication is laser-induced chemical liquid deposition (LCLD) of metals from deep eutectic solvents (DES), which was performed using continuous-wave (CW) lasers. In this work, we applied picosecond laser pulses and proposed a novel method for DES layer deposition to increase the speed and quality typical for LCLD methodology that uses the CW lasers. As a result, the fabrication speed of the conductive copper structures was increased up to 10 mm sec^{-1}. The electrical resistivity of these structures is 0.15 Ω mm^2 m^{-1}, which is the best result among similar structures previously obtained by LCLD. Moreover, this modified LCLD method does not need to use a vacuum chamber or photomask, while the DES preparation and deposition by spin-coating is very simple. In addition, there is no complexity and instability associated with the synthesis of the metallic nanostructured materials using the proposed methodology, which are typical for the conventional laser direct writing technology. Finally, there is no need to carry out the post-treatments such as sintering or additional cleaning steps. In order to show the high quality of the formed contacts, we demonstrate the stable and reproducible operation of the commercial light-emitting diodes connected by the contacts made by the proposed technique.

1. Introduction

In recent years, the demand for various optoelectronic devices such as liquid crystal displays, touch screens, solar cells, organic light-emitting diodes, and electrochromic devices [1] has significantly increased. The basis of their design is conductive coatings or conductive thin films, which are formed on different substrate surfaces. In turn, in comparison with traditional methods used for electrical contact fabrication such as photolithography and high-vacuum deposition techniques, the additive technologies are promising and rather cheap for manufacturing the conductive materials on different surfaces including flexible substrates [2].

Noble metals (Au, Ag) and ITO-based coatings are widely used for fabrication of the conductive contacts. However, due to the high cost of these materials, it is still an urgent task to reduce the expenses of the technological processes utilized for their production. On the other hand, copper attracts the attention of scientists and technologists as a worthy alternative to the aforementioned materials due to its low cost and excellent electrical conductivity. The electrical resistivity of copper (1.68 μΩ cm) is slightly lower than those of gold (2.21 μΩ cm), but the cost is 1000 times cheaper and accessibility is higher [3]. It is possible to distinguish three main groups among methods used for fabrication of the conductive copper patterns of the complicated geometry. The first group includes methods, in which the formation of a conductive layer on the substrate is followed by the removal of an excess of material. Such methods as direct current magnetron sputtering and high-power pulsed sputtering [4], chemical deposition from the gas phase [5] were developed and applied in industry, but it is necessary to use a multi-stage photolithography procedure to create a pattern. The second group includes methods that use templates or masks to create metal coatings. This group also includes screen printing, electrochemical deposition [6], chemical vapor deposition, and other sputtering methods. The main

* Corresponding authors.
E-mail addresses: i.i.tumkin@spbu.ru (I. Tumkin), lev.logunov@metalab.ifmo.ru (L. Logunov).

https://doi.org/10.1016/j.optlastec.2023.109777
Received 19 September 2022; Received in revised form 19 May 2023; Accepted 26 June 2023
Available online 20 July 2023

disadvantage of the second group is that one needs to create a new mask every time when you want to change the pattern, another disadvantage is the limitation of the width of the tracks due to edge effects. Finally, the third group includes technologies of frameless deposition: inkjet printing [7,8] and laser methods [9–11]. Examples of such laser methods are direct laser writing, laser direct patterning, laser selective patterning, and laser sintering [3,12], which showed relatively low cost, high productivity, relatively high environmental friendliness of the process, as well as do not require the use of traditional multi-stage photolithography processes, vacuum equipment, or high temperatures. Nevertheless, each of the laser methods has its advantages and disadvantages, which are discussed below.

Two-stage laser metallization technologies were proposed and developed in Refs [13–18]. Here, laser radiation plays the role of an "activator" to create a rough surface for chemical activation of the irradiated zones with subsequent chemical copper plating [14]. There is another technique, in which etching (activation) occurs with the help of absorbing material and subsequent chemical metallization (LIBWE) [19,20]. There are some limitations of such technology such as speed of scanning, type of surface, the thickness of the deposited structures, and possibility to deposit materials on each other. Also, it is still two-stage technology where one has to immerse samples into the solution for metallization [21].

Among the single-stage laser methods, it is necessary to note the advanced technologies of selective laser sintering that use precursors based on salts or nanoparticles of metal oxides. Examples of these methods are precision fabrication of copper micropatterns under the action of femtosecond near-IR radiation [22], and laser synthesis in the isolated system leading to fabrication of structures based on copper and nickel using CW laser [23]. However, this approach requires to apply the synthesized inks containing nanoparticles, which significantly increases the expanses.

The current work is focused on modification of the laser-induced chemical liquid deposition (LCLD) method [24–27], in which deposition of metallic layers and structures from solutions containing cheap and simple components occurs upon CW or pulsed radiation [28]. The advantages of this method are simplicity, low reagent consumption, the ability to control the shape and size of structures with an optical circuit, and the low cost of reagents. The main limitation of this method was the speed of fabrication, which did not allow scaling this technology. However, recently, it was shown that it is possible to increase the deposition rate of copper by an order of magnitude using deep eutectic solvents (DESs) as a medium for laser synthesis under visible CW laser irradiation [29,30]. Moreover, deep eutectic solvents have been gaining popularity for the last 10 years as "green" and safe to use solvents [31–33]. Such systems allow to create highly viscous solutions from two solids compounds and have the property of dissolving high concentrations of metal salts, which play an important role in the LCLD method. Nevertheless, so far, the relatively low speed (0.2 mm s^{-1}), relatively high resistivity, and a large number of structural defects of the deposited metal layers still prevent the practical application of the LCLD method in this regard.

In order to overcome the discussed problems concerning LCLD method, we performed copper deposition in a DES environment under the action of picosecond laser pulses, which reduce harmful overheating of the irradiated area during the process of laser-matter interaction. It is shown that the scanning speed, electrical conductivity, and geometric parameters of the resulting copper patterns are greatly influenced by both the parameters of laser radiation and the covering method (i.e. the thickness of a film containing DES components). We increased the scanning speed of individual lines of copper with the electrical resistivity of 0.13 Ω mm^2 m^{-1} by 50 times. Moreover, we developed a new method to control the thickness of the copper lines by using different thickness of the DES film. Previously, the preparation of a uniform DES film was a complex multi-stage process, including heating, covering of a film using spin coating, and final annealing [34,35]. The optimized LCLD method allows to demonstrate stable, and reproducible operation of commercial light-emitting diodes.

2. Experimental section

2.1. Materials and methods

Choline chloride, dihydrous copper(II) acetate ($Cu(Ac)_2{\cdot}2H_2O$, and citric acid were purchased from Sigma Aldrich (St. Louis, MO, USA) and used as received. Ultrapure Milli-Q water was used for the preparation of all water-containing solutions.

The choline chloride, citric acid, and copper(II) acetate were mixed in 10 mL glass vial. The molar composition of the mixture was 1:1:1 (choline chloride: citric acid: copper salt). Then, the vial was placed in a drying cabinet at 100 °C for 20 min. After the mixture began to melt, it was placed in a magnetic heating stirrer and mixed at 120° C until a viscous homogeneous liquid was formed. After this, the vial was air cooled and closed. The final solution was safely stored in a refrigerator for a few weeks. Before use in the deposition process, DES was heated in a drying cabinet at 100 °C for 15 min.

Sodium silicate glass was chosen as a substrate for deposition. The size of the substrates was 25 × 25 mm. The first and most important stage is the mechanical cleaning of glass in an aqueous solution of sodium hydroxide. After this, the substrate was sequentially washed in the running deionized water and in isopropyl alcohol. All samples were dried by blowing with atmospheric air at room temperature. All substrates were ozonated for 15 min for better adhesion of DES.

2.2. Des coating and laser-induced copper deposition

DES was dissolved in deionized water in a mass ratio of 3:1 (DES: Water). The ultrasonic bath was used to speed up the process. After dissolving, 100 μL of the resulting solution was spin coated on the previously cleaned glass. The speed of spin coating was changed for tuning of DES layer thickness. After spin coating, the substrates were immediately dried at 90 °C for 10 min on a hot plate.

The IR ATR spectra of the initial eutectic solvent, its mixture with water, and a thin film of DES after drying were recorded to confirm that the process of film preparation did not affect the structure of the original DES (Fig. 1a). As can be seen from the presented data, the IR spectra of the initial solvent and after drying practically coincide, while there is a slight shift in the region of 3200 cm^{-1}. This shift indicates a small change in hydrogen bonds, which may be associated with partial sorption of water in this solvent. However, the remaining positions of the bonds remained unchanged indicating only a minor change in the entire structure.

A picosecond laser (SOLAR LS) was used as a source of laser irradiation with the following parameters: wavelength of 1064 nm, pulse duration of 7 ps, repetition rate of 80 MHz, and average power was varied from 0.1 to 5 W. Laser irradiation was focused and controlled using galvo-scanner system. The diameter of the focal spot was approximately 20 μm. The scanning speed was changed from 0.1 to 10 mm s^{-1}. A software of the galvo-scanner allows to create patterns of any geometry on the surface of substrates. All steps of the fabrication are presented in Fig. 1b. A schematic of the laser writing setup is available in Fig S1. The protocol starts with covering the substrate with DES. Then, laser-induced synthesis is followed by rinsing of the substrate with deionized water several times, 0.1 M sodium carbonate solution and once more with deionized water.

2.3. Method of analysis

Sem/Afm/Optical microscope

Morphology of the obtained materials were studied using scanning electron microscopy (Merlin,Carl Zeiss) and Scanning Probe Microscopy (SmartSPM, HORIBA France SAS). An AXIO IMAGER VARIO A2M

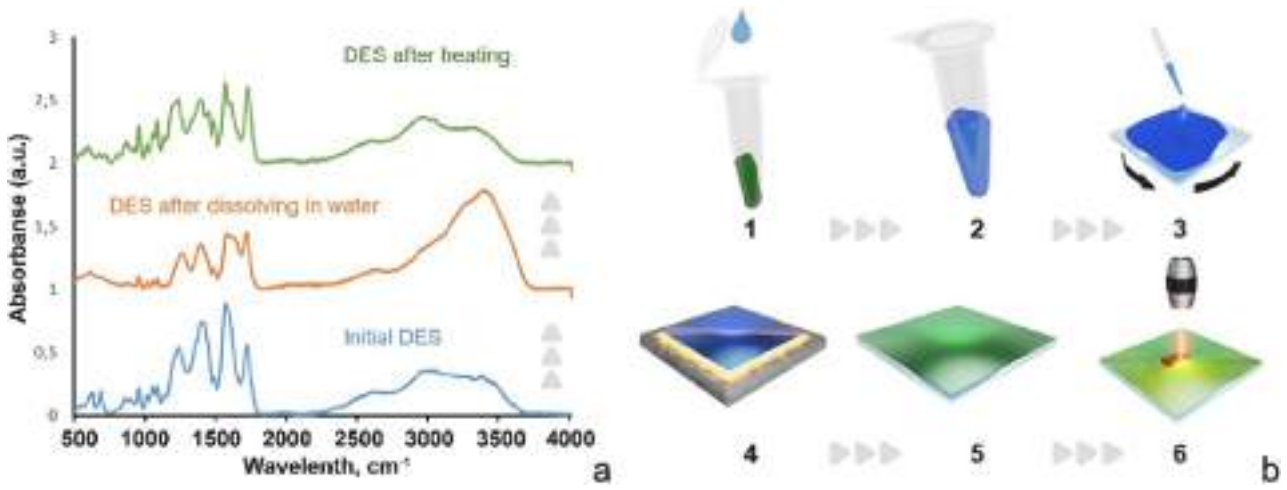

Fig. 1. Principle of direct laser writing of electrodes. (a) IR ATR spectra of DES (1-DES, 2-DES with water, 4-dried film of DES solution). (b). Steps of laser-induced deposition of copper patterns (1-DES, 2-DES with adds of water, 3-wet film of DES solution applied by spin-coating, 4-dried film of DES solution, 5-laser patterning, 6-washed sample).

microscope was used to evaluate the samples in the visible range.

Profilometer

Cross-section measurements for electrical resistivity calculations were conducted using the KLA Tencor P-7 profilometer (sampling step is 4 A, the minimum impact of the stylus equals 0.05 mg).

Uv/Ir spectroscopy

Absorption and infrared spectra of DES solutions were collected by Shimadzu spectrophotometers UV-3600 Plus and IRPrestige-21.

Xrd analysis

The phase composition of the fabricated patterns was evaluated by X-ray diffraction on a Shimadzu XRD-7000 Maxima diffractometer with a source of monochromatic Cu-kα radiation with a wavelength of 0.15406 nm. The diffraction patterns were taken in the Bragg-Brentano geometry with a step $\theta = 0.01^{\circ}$.

Xps analysis

The surface composition of the fabricated materials was determined by X-ray photoelectron spectroscopy (XPS) on a Thermo Scientific "K-Alpha" spectrometer with an Al-kα monochromatic radiation source ($E = 1.486$ keV).

3. Results and discussion

In our experiments, we used a three-component deep eutectic solvent based on choline chloride/citric acid/copper(II) acetate with a molar ratio of 1:1:1. Quantitative composition was chosen according to our previous studies [30]. As for metal precursor, a lower copper salt content in the final solution was insufficient for the fabrication of continuous conductive structures. On the other hand, a higher copper acetate concentration led to formation of heterogeneous systems with inclusions of the undissolved salt crystals in the saturated DES. Deposition from such solutions resulted in manufacturing the defective structures with high electrical resistance. As for the proton acceptor of the DES, choline chloride is the most commonly used component due to its low cost and sustainability. Citric acid was found to be an optimal choice for proton donor since it reveals a high reduction ability of copper ions under the condition of laser-induced synthesis and forms suitable DES in terms of viscosity and adhesion to dielectric substrates [29]. In this study, copper (II) chloride was replaced by copper(II) acetate, since this chemical is commercially available at a low cost in the form of two molecules of water of crystallization (compared to chloride with six molecules of water of crystallization). Lower water content in salt crystals allows to produce DES with a reduced amount of water in the final solution without additional laborious stages of synthesis. Such systems exhibit more preferable physical parameters for laser fabrication including viscosity and adhesion. In addition, copper(II) acetate is more photoactive than chloride. This fact opens up the possibility of using picosecond radiation with a lower average power density compared to CW laser light previously used for thermally-induced synthesis from DES [36]. This allowed to significantly accelerate the deposition procedure compared to our previous experiments.

The laser-induced deposition technique is based on the interaction of a laser beam with the surface of the substrate under a layer of precursor (DES in the present case). As a result of photo- and thermal processes localized within the laser focal point, chemical reaction of metal reduction occurs. Scanning the surface with the focused laser beam leads to fabrication of metal patterns. The width of the fabricated structures is 2–3 times wider than the focal spot, which argues in favor of the thermal mechanism predominance. More detailed discussion and some mechanistic ideas of copper reduction in DES and water-based systems were reported elsewhere for continuous wave (cw) laser irradiation [25,36–38]. The direct measurements of temperature within the focus of the laser beam are quite difficult to perform due to the micro-dimensional size of the area and non-equilibrium processes occurring during the laser exposure. Due to high temperature, the majority of side products evaporate and the deposited metal stays on the substrate in the form of a line. The profile of the fabricated copper patterns is most likely caused by local overheating in the center of the line (Fig. 2b). The morphology of the patterns fabricated with different energies was studied by SEM (Fig. 2d and e; Fig. S2 and Fig. S4). Two characteristic areas are noticeable: a relatively flat middle part and high lateral regions, which is in agreement with the data acquired by AFM and profilometry (Fig. 2). EDX element mapping is shown in SI (Fig. S4.). The film has a highly porous structure with a wide size distribution from tenths to a few microns (Fig. 2e). The copper based materials with such architecture are promising for manufacturing the microelectrodes for electrochemical sensors [39–41]. Moreover, the laser-assisted fabrication technique allows to deposit microelectrodes on any arbitrary surfaces without a mask or any other additional technological requirements.

One of the functional properties of copper patterns crucial for practical application is high electrical conductivity. As a result, such physical parameters as power density, scan speed, and DES film thickness were optimized for fabrication of copper structures with low electrical resistance. The thickness of the DES film on the glass was controlled by the spin-coating speed. For 1000, 2000, 3000, and 4000 rpm films thickness were of 15, 11, 8, and 7 μm, respectively (Fig. S5). A further increasing speed of spin coating did not lead to thinning the film of DES, which is associated with drying of water from the solution and a strong increase

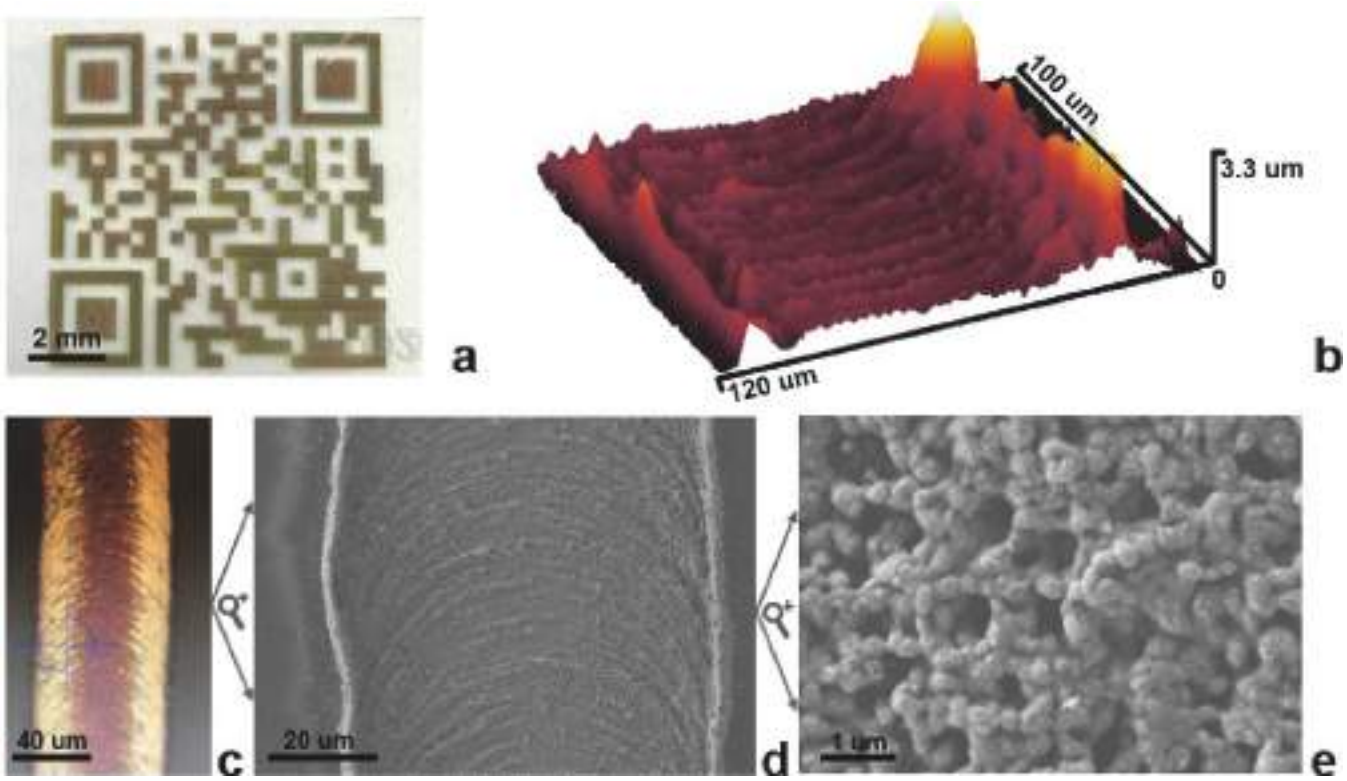

Fig. 2. Copper electrodes morphology characterization. (a) Optical image of copper patterns on the glass. (b) The cross-section of the fabricated copper pattern. (c-e) SEM images of copper patterns (scale bar on image).

in the viscosity of the solution during the spin-coating process. The proposed procedure of DES film manufacturing can find application not only in the laser-assisted fabrication of functional materials but can be useful for electrodeposition [42], membrane coating [35], etc.

The cross-section of copper patterns was studied by the AFM and stylus profilometer method for resistivity calculations (Fig. 2). The profile has characteristic areas: a relatively flat middle part and side peaks, which are explained by high temperatures in the center of the focal spot. Patterns at fixed laser deposition parameters were fabricated for DES film thickness optimization. Films with lower thickness tend to decrease side peaks while maintaining the height of the middle area (Fig. 3). The dependence of the copper pattern width on the laser radiation power density for different DES thicknesses is shown in Fig. 3a. The laser scanning speed was selected experimentally and for all studies was 2.5 mm s^{-1}. It is worth noting that this is 10 times faster than those for our previous works [25,27,37,38].

Change in the power density of laser radiation shows similar changes in the width of copper patterns for different thicknesses of DES on the glass substrate (Fig. 3a). There are three characteristic zones of width dependence:

1. The first zone of low power (less than 14 kW cm^{-2}) demonstrates a linear increasing the width of the copper pattern, regardless of the thickness of the DES film. The quality of the deposited patterns is extremely low, gaps and defects are observed. The speed of increase of width for 15 μm DES is 882 nm/(kW cm^{-2}), for others – 705 nm/(kW cm^{-2}).
2. The second zone lies between 14 and 40 kW cm^{-2}. Dependencies for all thicknesses differ significantly:
   - For the 15 μm DES film dependence changes from linear to parabolic.
   - The width of copper patterns grows faster for the 11 μm DES film than those for the 8 μm DES due to difference in the film thicknesses, but the dependence does not fundamentally change.
   - The width of copper patterns reaching 100 μm for 7 μm DES film does not change with an increase in the radiation power density, since the film thickness is not enough to increase the width.
3. The third zone starts from 40 kW cm^{-2}, and for all film thicknesses is characterized by a sharp increase in width. At the same time, the number of defects increases dramatically (geometry deformation - local narrowing and broadening), in addition, ablation occurs in the center of the pattern.

Optical and SEM images of the structures obtained at different power densities are given in the SI (Fig. S2).

Actually, the adhesion of metal to substrate is one of the major characteristics when the deposition or sputtering techniques are applied. As has been suggested previously[43], solution components can react with multi-component glass under extreme laser irradiation conditions to form a chemically bonded layer, which is also favorable for strong metal-to-glass adhesion. On the other hand for ps laser pulses the multiphoton and tunnel ionization mechanisms (dominating for fs laser pulses) are extended by impact ionization due to the electrons accelerated in the electric field [44,45]. Thus, we speculate that the copper particles are heated by the laser beam and partly melt into the glass substrate. This provides certain bonding between the laser-written copper pattern and glass substrate. However, further research is still ongoing to better understand the nature of the adhesion of laser-deposited copper micropatterns.

The electrical resistance was measured by a two-probe method. The cross-section of the conductor was calculated using data, which was obtained by stylus profilometry. Finally, the obtained values were converted into the electrical resistivity ones (Fig. 3c and d). The applied copper pattern for the resistance measurements had a rectangle shape with sides of 8 × 2 mm. The silver paste was placed on the short sides to minimize contact losses. Ten measurements of each regime were carried out for the error determination.

The dependence of the electrical resistivity of copper patterns on

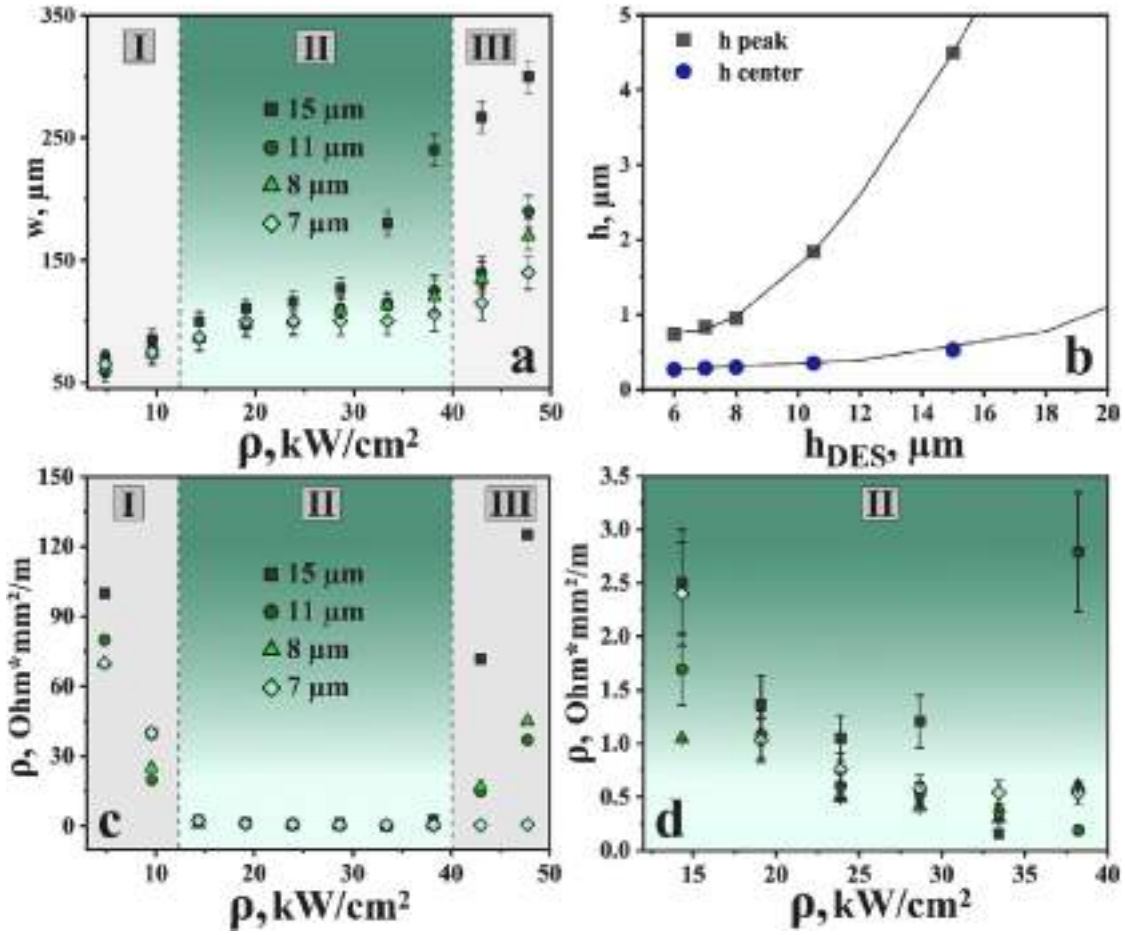

Fig. 3. Electrodes deposition optimization. (a) Dependence of the copper pattern width on laser power density (points); (b) Dependence of the height of the middle and side peaks of copper patterns on the DES thickness at the fixed radiation power; (c) Dependence of the electrical resistivity on laser power density; (d) Dependence of the electrical resistivity on laser power density in zone II.

laser power density can be also distinguished in the following characteristic zones:

In the first zone, the electrical resistivity decreases from 80 to 100 to 1–3 Ω mm^2 m^{-1} due to increasing the cross-section of copper patterns.

In the second zone, we obtained minimal values of the electrical resistivity for all thicknesses of the DES films: 0.15 (for the 15 μm DES), 0.18 (for the 11 μm DES), 0.3 (for the 8 μm DES), and 0.5 (for the 7 μm DES) Ω mm^2 m^{-1}. The optimal thickness of the DES film varied from 15 to 11 μm. It was possible to obtain a minimum number of defects on copper patterns using such films.

In the third zone, the electrical resistance grew rapidly up to hundreds of Ω mm^2 m^{-1}, which is associated with the ablation of a part of the material in the center of the copper pattern and formation of a large number of defects on its edge parts (Fig. S2).

To exclude the fact that the changes in the electrical resistances were referred to a change in the composition of copper structures, the phase composition was studied by XRD analysis. Fig. S6 shows a series of XRD patterns for five samples fabricated at different metallization regimes. It is clear that in all cases, there is the same number of reflections corresponding to the reflection angles (111), (200) and (220) of metallic copper [46]. Minor deviations in the ratios of reflection intensities exclude the formation of texture and micro stresses in the patterns, which implies high reproducibility of the proposed fabrication technique.

The most optimal parameters used for the synthesis of copper patterns with the least number of defects are the thickness of the DES film of 11 μm, power density of 37 kW cm^{-2} and scanning speed of 2.5 mm s^{-1}. Using such conditions, it was possible to obtain copper deposits with an electrical resistivity of about 0.18 Ω mm^2 m^{-1}. Thus, the proposed experimental approach allowed to draw complicated patterns at high speed using any vector image. The examples of different copper drawings on the glass surface and an electrical circuit assembled with the connection of FM-3528HYK-589O and BL-LS3014A0S1UW2C diodes are presented in Fig. 4.

We carried out an XPS analysis of the fabricated copper patterns. The central part and the edge peak of the pattern were separately identified as areas of interest. The spectra were recorded under conditions of ultrahigh vacuum $2{\cdot}10^{-9}$ mBar. The high-resolution spectra of C1s, O1s, N1s, and Cu2p photoelectron lines were obtained in the constant transmission energy mode (pass energy = 20 eV, with a step of 0.1 eV).

The XPS analysis showed that copper patterns contain carbon, oxygen, nitrogen, and copper. According to the sample composition analysis (Fig. S7), it can be concluded that the basis of the pattern surface is carbon and oxygen. To elucidate the reason for such an amount of carbon and oxygen, component analysis of the high-resolution spectra of C1s, O1s, N1s, and Cu2p photoelectron lines was carried out. The shape of the C1s photoelectron line (Fig. 5a) confirms not only the presence of carbon adsorbed from the atmosphere on the surface of the sample but also the formation of carbonyl groups as shown by the characteristic component for metal carbonates with the binding energy (BE) of 288.7 eV [47]. In addition, line broadening in the region of 286–288 eV also

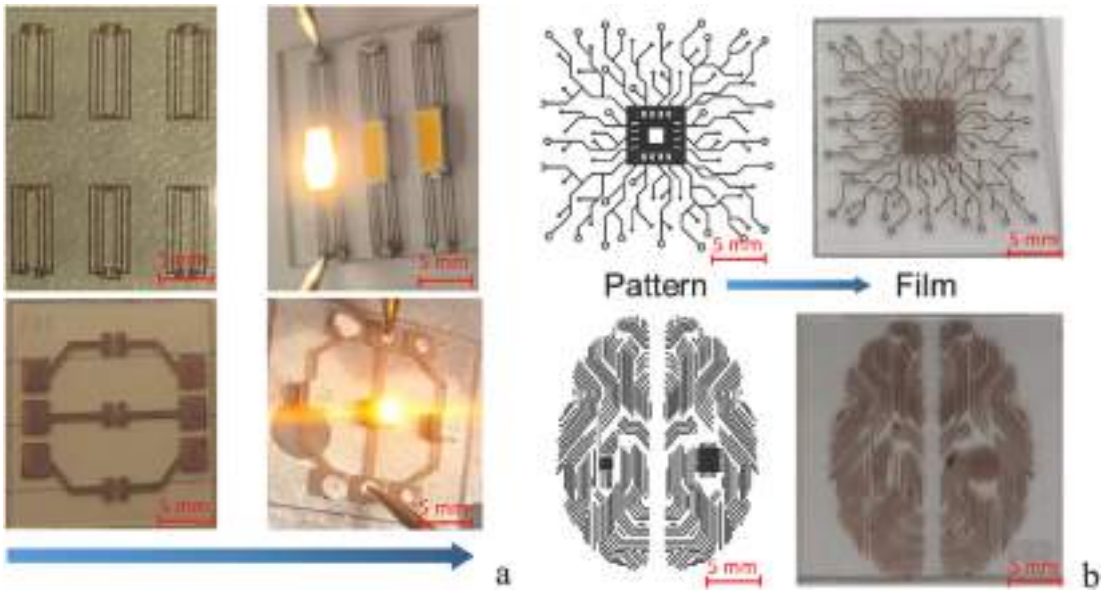

Fig. 4. Electrodes application for light-emitting devices. (a) Different copper patterns on glass (left), LED connection using deposited copper (right); (b) Copper patterns drawn in Corel Draw (left) and deposited from DES (right).

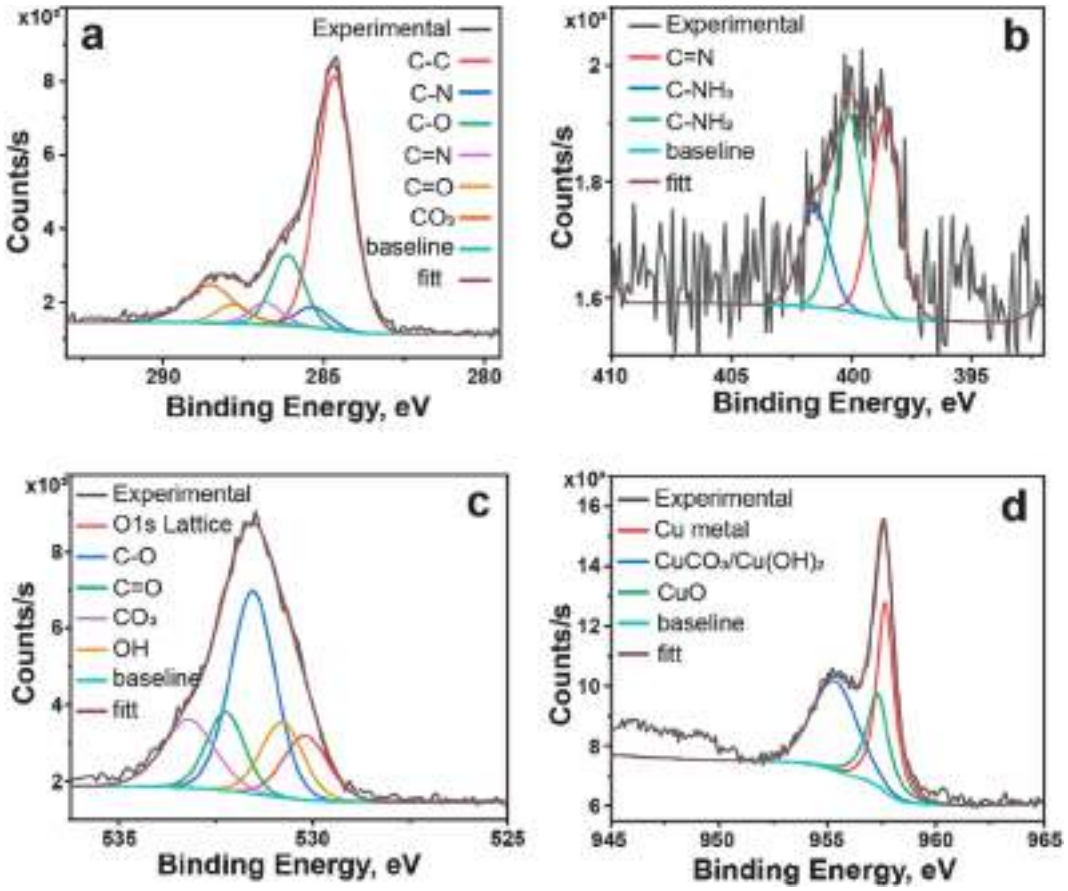

Fig. 5. X-ray photoemission spectroscopy for composition analysis of the electrodes. The element percentages along the fabricated copper pattern are shown in the insert. (a-d) High resolution spectra of C1s, O1s, N1s, and Cu2p3 photoemission core lines.

indicates the presence of carbon–nitrogen bonds, which correspond to C–N (285.6 eV) and C = N (286.9 eV) bonds, respectively [48]. Deconvolution of the high-resolution spectrum of the N1s photoelectron line (Fig. 5b) confirms the presence of C-N and C = N bonds on the surface of the sample. The shape, position of the O1s photoelectronic line (Fig. 5c) indicates the presence of both carboxylic oxides and metal oxide, in particular copper(II) oxide [49,50]. An analysis of the Cu2p3 photoelectronic line (Fig. 5d) qualitatively proves not only the presence

of copper(II) oxide but also copper(II) carbonate on the surface of the sample [51]. It is clear that the number of metal bonds and carboxyl bonds is quite close for the photoelectron line of copper, while the oxide component is almost half as much (Fig. S7). The formation of these compounds on the surface is quite due to the peculiarities of the synthesis. In the first stage, as a result of laser exposure, high temperatures are reached, metallic copper is formed from the organic complex, and part of the reaction products further interacts with heated copper. As the beam moves, under atmospheric conditions, the metal is locally cooled to temperatures, when oxidative reactions begin with formation of copper oxide on its surface. It should be noted that these species are formed only on the surface of the metallic deposit as evidenced by the intense signal of metallic copper in the XPS (Fig. 5d).

4. Conclusion

In this work, we have demonstrated the possibility to perform deposition of high-quality conductive copper coatings from deep eutectic solvents using picosecond laser irradiation. We found the parameters of the deposition regime, at which the final electrical resistance reached value at 7 times higher of a bulk copper. The minimum geometric dimensions of a single line are about 90 μm in width and a few of microns in height. The quality and morphology of the coating indicate the possibility of increasing the deposition rate. As a result, the developed approach overcomes the previous limitations of the one-stage laser-assisted deposition technology, and opens the opportunities for new applications of this method, e.g. in micro-LEDs and displays technologies. We anticipate further development of this approach for fabrication of a wide range of conductive materials on various substrates with higher deposition rate. In further research the resolution of the pattern can be improved by better focusing of the laser light. The reduction of the wavelength of the laser will on the one hand reduce the laser spot size, but on the other hand, change the absorption coefficients and can therefore completely change the physical picture of the laser writing process. Application of optics with a higher numerical aperture will enable a tighter focusing and hence improve the resolution without changing the laser wavelength.

CRediT authorship contribution statement

Dmitry Shestakov: Methodology, Investigation, Data curation. **Evgeniia Khairullina:** Formal analysis, Investigation, Data curation, Writing – original draft, Visualization. **Andrey Shishov:** Conceptualization, Methodology, Formal analysis. **Soslan Khubezhov:** Data curation, Visualization, Visualization. **Sergey Makarov:** Writing – review & editing, Project administration, Funding acquisition. **Ilya Tumkin:** Conceptualization, Writing – original draft, Writing – review & editing, Supervision, Funding acquisition. **Lev Logunov:** Conceptualization, Methodology, Investigation, Data curation, Writing – original draft, Writing – review & editing, Supervision, Project administration.

Declaration of Competing Interest

The authors declare that they have no known competing financial interests or personal relationships that could have appeared to influence the work reported in this paper.

Data availability

Data will be made available on request.

Acknowledgements

I.I.T. and E.M.K. acknowledge the Russian Science Foundation's (grant 20-79-10075) support for the design of chemical compositions for the selective metallization and laser fabrication of patterns. M.S.V. and L.L. are thankful to the Ministry of Science and Higher Education of the Russian Federation (Project 075-15-2021-589) for supporting the experiments on layers characterization and application for devices.. The authors would like to thank the SPbSU Nanotechnology Interdisciplinary Centre, Centre for Optical and Laser Materials Research, and ITMO Core Facility Center "Nanotechnologies".

Appendix A. Supplementary data

Supplementary data to this article can be found online at https://doi.org/10.1016/j.optlastec.2023.109777.

References

[1] D. Won, J. Kim, J. Choi, H. Kim, S. Han, I. Ha, J. Bang, K.K. Kim, Y. Lee, T. Kim, J. Park, C. Kim, S.H. Ko, Digital selective transformation and patterning of highly conductive hydrogel bioelectronics by laser-induced phase separation, Sci. Adv. 8 (2022) eabo3209, https://doi.org/10.1126/sciadv.abo3209.
[2] M.E.H. Bhuiyan, A. Behroozfar, S. Daryadel, S. Moreno, S. Morsali, M. Minary-Jolandan, A hybrid process for printing pure and high conductivity nanocrystalline copper and nickel on flexible polymeric substrates, Sci. Rep. 9 (2019) 1–10, https://doi.org/10.1038/s41598-019-55640-7.
[3] V.B. Nam, T.T. Giang, S. Koo, J. Rho, D. Lee, Laser digital patterning of conductive electrodes using metal oxide nanomaterials, Nano Converg. 7 (2020) 23, https://doi.org/10.1186/s40580-020-00232-9.
[4] I.L. Velicu, V. Tiron, B.G. Rusu, G. Popa, Copper thin films deposited under different power delivery modes and magnetron configurations: A comparative study, Surf. Coatings Technol. 327 (2017) 192–199, https://doi.org/10.1016/j.surfcoat.2016.11.001.
[5] N. Prud'homme, V. Constantoudis, A.E. Turgambaeva, V.V. Krisyuk, D. Samélor, F. Senocq, C. Vahlas, Chemical vapor deposition of Cu films from copper(I) cyclopentadienyl triethylphophine: Precursor characteristics and interplay between growth parameters and films morphology, Thin Solid Films. 701 (2020) 137967, https://doi.org/10.1016/j.tsf.2020.137967.
[6] Y.C. Liao, Z.K. Kao, Direct writing patterns for electroless plated copper thin film on plastic substrates, ACS Appl. Mater. Interfaces. 4 (2012) 5109–5113, https://doi.org/10.1021/am301654j.
[7] S. Naghdi, K.Y. Rhee, D. Hui, S.J. Park, A review of conductive metal nanomaterials as conductive, transparent, and flexible coatings, thin films, and conductive fillers: Different deposition methods and applications, Coatings. 8 (2018) 1–27, https://doi.org/10.3390/coatings8080278.
[8] A. Albrecht, A. Rivadeneyra, A. Abdellah, P. Lugli, J.F. Salmerón, Inkjet printing and photonic sintering of silver and copper oxide nanoparticles for ultra-low-cost conductive patterns, J. Mater. Chem. C. 4 (2016) 3546–3554, https://doi.org/10.1039/c6tc00628k.
[9] S. Jung, J.M. Lee, Y. Han, J.H. Kim, R. Hidayati, J. Rhyee, W.N. Kang, W.S. Choi, H. Jeon, J. Suk, T. Park, High critical current density and high-tolerance superconductivity in high-entropy alloy thin films, Nat. Commun. 13 (2022) 3373, https://doi.org/10.1038/s41467-022-30912-5.
[10] C. Yifan, S.F. Hung, W.K. Lo, Y. Chen, Y. Shen, K. Kafenda, J. Su, K. Xia, S. Yang, A universal method for depositing patterned materials in situ, Nat. Commun. 11 (2020) 5334, https://doi.org/10.1038/s41467-020-19210-0.
[11] B. Deore, K.L. Sampson, T. Lacelle, N. Kredentser, J. Lefebvre, L.S. Young, J. Hyland, R.E. Amaya, J. Tanha, P.R.L. Malenfant, H.W. De Haan, C. Paquet, Direct printing of functional 3D objects using polymerization-induced phase separation, Nat. Commun. 12 (2021) 55, https://doi.org/10.1038/s41467-020-20256-3.
[12] J. Kwon, H. Cho, Y.D. Suh, J. Lee, H. Lee, J. Jung, D. Kim, D. Lee, S. Hong, S.H. Ko, Flexible and transparent Cu electronics by low-temperature acid-assisted laser processing of Cu nanoparticles, Adv. Mater. Technol. (2016) 1600222, https://doi.org/10.1002/admt.201600222.
[13] H. Xu, J. Zhang, J. Feng, T. Zhou, Fabrication of copper patterns on polydimethylsiloxane through laser-induced selective metallization, Ind. Eng. Chem. Res. 60 (2021) 8821–8828, https://doi.org/10.1021/acs.iecr.1c01668.
[14] J. Zhang, J. Feng, L. Jia, H. Zhang, G. Zhang, S. Sun, T. Zhou, Laser-Induced selective metallization on polymer substrates using organocopper for portable electronics, ACS Appl. Mater. Interfaces. 11 (2019) 13714–13723, https://doi.org/10.1021/acsami.9b01856.
[15] J. Zhang, Y. Xie, H. Xu, T. Zhou, Efficient and simple fabrication of high-strength and high-conductivity metallization patterns on flexible polymer films, Ind. Eng. Chem. Res. 61 (2022) 6987–6996, https://doi.org/10.1021/acs.iecr.2c00850.
[16] Y. Ji, Y. Liao, H. Li, Y. Cai, D. Fan, Q. Liu, S. Huang, R. Zhu, S. Wang, H. Wang, G. Liang, Flexible metal electrodes by femtosecond laser-activated deposition for human-machine interfaces, ACS Appl. Mater. Interfaces. 14 (2022) 11971–11980, https://doi.org/10.1021/acsami.2c00419.
[17] V. Fiodorov, K. Ratautas, Z. Mockus, R. Trusovas, L. Mikoliūnaitė, G. Račiukaitis, Laser-assisted selective fabrication of copper traces on polymers by electroplating, Polymers (Basel). 14 (2022) 791, https://doi.org/10.3390/polym14040781.
[18] H.-J. Huang, M.-B. Zhou, X.-P. Zhang, Ingenious method for rapid fabrication of a highly conductive hybrid film of printed Cu Nanoparticle layers plated by Ag nanoplates on a PET substrate at room temperature, ACS Appl. Electron. Mater. 3 (2021) 4640–4648, https://doi.org/10.1021/acsaelm.1c00804.

[19] J.M. Seo, K.K. Kwon, K.Y. Song, C.N. Chu, S.H. Ahn, Deposition of durable micro copper patterns into glass by combining laser-induced backside wet etching and laser-induced chemical liquid phase deposition methods, Materials (Basel). 13 (2020) 1–13, https://doi.org/10.3390/ma13132977.
[20] J. Long, J. Li, M. Li, X. Xie, Fabrication of robust metallic micropatterns on glass surfaces by selective metallization in laser-induced porous surface structures, Surf. Coatings Technol. 374 (2019) 338–344, https://doi.org/10.1016/j.surfcoat.2019.06.018.
[21] S. Jo, S. Akin, M.S. Park, M.B.G. Jun, Selective metallization on glass surface by laser direct writing combined with supersonic particle deposition, Manuf. Lett. 31 (2022) 64–68, https://doi.org/10.1016/j.mfglet.2021.07.009.
[22] M. Mizoshiri, T. Hayashi, J. Narushima, T. Ohishi, Femtosecond laser direct writing of Cu–Ni alloy patterns in ambient atmosphere using glyoxylic acid Cu/Ni mixed complexes, Opt. Laser Technol. 144 (2021) 107418, https://doi.org/10.1016/j.optlastec.2021.107418.
[23] V. Binh Nam, T. Thi Giang, D. Lee, Laser digital patterning of finely-structured flexible copper electrodes using copper oxide nanoparticle ink produced by a scalable synthesis method, Appl. Surf. Sci. 570 (2021) 151179, https://doi.org/10.1016/j.apsusc.2021.151179.
[24] Y. Huang, X. Xie, J. Cui, W. Zhou, J. Chen, J. Long, Robust metallic micropatterns fabricated on quartz glass surfaces by femtosecond laser-induced selective metallization, Opt. Express. 30 (2022) 19544, https://doi.org/10.1364/oe.456927.
[25] M.S. Panov, A.E. Grishankina, D.D. Stupin, A.I. Lihachev, V.N. Mironov, D. M. Strashkov, E.M. Khairullina, I.I. Tumkin, M.N. Ryazantsev, In situ laser-induced fabrication of a ruthenium-based microelectrode for non-enzymatic dopamine sensing, Materials (Basel). 13 (2020) 1–11, https://doi.org/10.3390/ma13235385.
[26] M. Cui, T. Huang, R. Xiao, Rapid fabrication of conductive copper patterns on glass by femtosecond Laser-Induced reduction, Appl. Surf. Sci. 588 (2022) 152915, https://doi.org/10.1016/j.apsusc.2022.152915.
[27] M.S. Panov, E.M. Khairullina, F.S. Vshivtcev, M.N. Ryazantsev, I.I. Tumkin, Laser-induced synthesis of composite materials based on iridium, gold and platinum for non-enzymatic glucose sensing, Materials (Basel). 13 (2020) 1–11, https://doi.org/10.3390/ma13153359.
[28] H.G. Kim, M.S. Park, Fast fabrication of conductive copper structure on glass material using laser-induced chemical liquid phase deposition, Appl. Sci. 11 (2021), https://doi.org/10.3390/app11188695.
[29] A. Shishov, D. Gordeychuk, L. Logunov, A. Levshakova, E. Andrusenko, I. Chernyshov, E. Danilova, M. Panov, E. Khairullina, I. Tumkin, Laser-induced deposition of copper from deep eutectic solvents: optimization of chemical and physical parameters, New J. Chem. 45 (2021) 21896–21904, https://doi.org/10.1039/d1nj04158d.
[30] A. Shishov, D. Gordeychuk, L. Logunov, I. Tumkin, High rate laser deposition of conductive copper microstructures from deep eutectic solvents, Chem. Commun. 55 (2019) 9626–9628, https://doi.org/10.1039/c9cc05184h.
[31] E.L. Smith, A.P. Abbott, K.S. Ryder, Deep eutectic solvents (DESs) and Their applications, Chem. Rev. 114 (2014) 11060–11082, https://doi.org/10.1021/cr300162p.
[32] B.B. Hansen, S. Spittle, B. Chen, D. Poe, Y. Zhang, J.M. Klein, A. Horton, L. Adhikari, T. Zelovich, B.W. Doherty, B. Gurkan, E.J. Maginn, A. Ragauskas, M. Dadmun, T.A. Zawodzinski, G.A. Baker, M.E. Tuckerman, R.F. Savinell, J. R. Sangoro, Deep eutectic solvents: A review of fundamentals and applications, Chem. Rev. 121 (2021) 1232–1285, https://doi.org/10.1021/acs.chemrev.0c00385.
[33] Q. Zhang, K. De Oliveira Vigier, S. Royer, F. Jerome, Deep eutectic solvents: syntheses, properties and applications, Chem. Soc. Rev. 41 (2012) 7108–7146, https://doi.org/10.1039/c2cs35178a.
[34] M.H. Rahman, S. Ahmmed, S. Tabassum, A.B.M. Ismail, Epitaxial deposition of LaF3thin films on Si using deep eutectic solvent based facile and green chemical route, AIP Adv. 11 (2021) 035010, https://doi.org/10.1063/5.0039733.
[35] M. Mohammadi, M.B. Karimi, F. Mohammadi, S. Mehdipour-Ataei, Anhydrous proton conductivity of sulfonated polysulfone/deep eutectic solvents (DESs) composite membranes: Effect of sulfonation degree and DES composition, Int. J. Hydrogen Energy. 47 (2022) 1132–1143, https://doi.org/10.1016/j.ijhydene.2021.10.056.
[36] A.S. Levshakova, E.M. Khairullina, L.S. Logunov, M.S. Panov, A.S. Mereshchenko, V.B. Sosnovsky, D.I. Gordeychuk, A. Yu, I.I. Tumkin, Highly rapid direct laser fabrication of Ni micropatterns for enzyme-free sensing applications using deep eutectic solvent, Mater. Lett. 308 (2022) 131085, https://doi.org/10.1016/j.matlet.2021.131085.
[37] L.S. Logunov, M.S. Panov, L.A. Myund, I.I. Tumkin, E.M. Khairullina, M. N. Ryazantsev, I.A. Balova, V.A. Kochemirovsky, Influence of the ligand nature on the in situ laser-induced synthesis of the electrocatalytically active copper microstructures, Arab. J. Chem. 11 (2018) 624–634, https://doi.org/10.1016/j.arabjc.2017.11.003.
[38] V.A. Kochemirovsky, L.S. Logunov, S.V. Safonov, I.I. Tumkin, Y.S. Tver'Yanovich, L.G. Menchikov, Sorbitol as an efficient reducing agent for laser-induced copper deposition, Appl. Surf. Sci. 259 (2012) 55–58, https://doi.org/10.1016/j.apsusc.2012.06.085.
[39] E.M. Khairullina, K. Ratautas, M.S. Panov, V.S. Andriianov, S. Mickus, A. A. Manshina, G. Račiukaitis, I.I. Tumkin, Laser - assisted surface activation for fabrication of flexible non - enzymatic Cu - based sensors, Microchim. Acta. 189 (2022) 259, https://doi.org/10.1007/s00604-022-05347-w.
[40] V.B. Juska, A. Walcarius, M.E. Pemble, A. Walcarius, M.E. Pemble, Cu Nanodendrite foams on integrated band array electrodes for the nonenzymatic detection of glucose, ACS Appl. Nano Mater. 2 (2019) 5878–5889, https://doi.org/10.1021/acsanm.9b01325.
[41] N. Zhang, J. Yang, C. Hu, Laser-scribed graphene sensors on nail polish with tunable composition for electrochemical detection of nitrite and glucose, Sensors Actuators B. Chem. 357 (2022) 131394, https://doi.org/10.1016/j.snb.2022.131394.
[42] C. Liu, J. Qi, B. He, H. Zhang, J. Ju, X. Yao, Ionic conductive gels based on deep eutectic solvents, Int. J. Smart Nano Mater. 12 (2021) 337–350, https://doi.org/10.1080/19475411.2021.1972053.
[43] T. Lipateva, A. Lipatiev, S. Lotarev, G. Shakhgildyan, S. Fedotov, V. Sigaev, One-stage femtosecond laser-assisted deposition of gold micropatterns on dielectric substrate, Materials (Basel). 15 (2022), https://doi.org/10.3390/ma15196867.
[44] I. Mirza, N.M. Bulgakova, J. Tomáštík, V. Michálek, O. Haderka, L. Fekete, T. Mocek, Ultrashort pulse laser ablation of dielectrics: Thresholds, mechanisms, role of breakdown, Sci. Rep. 6 (2016) 1–11, https://doi.org/10.1038/srep39133.
[45] B. Rethfeld, Free-electron generation in laser-irradiated dielectrics, Contrib. to, Plasma Phys. 47 (2007) 360–367, https://doi.org/10.1002/ctpp.200710048.
[46] H.E. Swanson, H.F. McMurdie, M.C. Morris, E.H. Evans, Standard X-ray Diffraction Powder Patterns, National Bureau of Standards (U.S.), 1967.
[47] S. Gu, C. Te Hsieh, T.W. Lin, C.Y. Yuan, Y. Ashraf Gandomi, J.K. Chang, J. Li, Atomic layer oxidation on graphene sheets for tuning their oxidation levels, electrical conductivities, and band gaps, Nanoscale. 10 (2018) 15521–15528, https://doi.org/10.1039/c8nr04013c.
[48] R. Vajtai, Springer handbook of nanomaterials, springer-Verlag, Berlin Heidelberg (2013), https://doi.org/10.1007/978-3-642-20595-8.
[49] I. Platzman, R. Brener, H. Haick, R. Tannenbaum, Oxidation of polycrystalline copper thin films at ambient conditions, J. Phys. Chem. C. 112 (2008) 1101–1108, https://doi.org/10.1021/jp076981k.
[50] Y. Wang, Y. Lü, W. Zhan, Z. Xie, Q. Kuang, L. Zheng, Synthesis of porous Cu2O/CuO cages using Cu-based metal-organic frameworks as templates and their gas-sensing properties, J. Mater. Chem. A. 3 (2015) 12796–12803, https://doi.org/10.1039/c5ta01108f.
[51] F. Liu, L. Csetenyi, G.M. Gadd, Amino acid secretion influences the size and composition of copper carbonate nanoparticles synthesized by ureolytic fungi, Appl. Microbiol. Biotechnol. 103 (2019) 7217–7230, https://doi.org/10.1007/s00253-019-09961-2.